2013-10-01

PDMS Based Coplanar Microfluidic Channels for the Surface Reduction of Oxidized Galinstan

UTD AUTHOR(S): Daeyoung Kim and Jeong-Bong Lee

Lab on a Chip

PAPER

View Article Online
View Journal | View Issue

PDMS based coplanar microfluidic channels for the surface reduction of oxidized Galinstan†

Cite this: *Lab Chip*, 2014, **14**, 200

Guangyong Li,[a] Mitesh Parmar,[a] Daeyoung Kim,[b] Jeong-Bong (JB) Lee[b] and Dong-Weon Lee*[a]

Received 16th August 2013,
Accepted 1st October 2013

DOI: 10.1039/c3lc50952d

www.rsc.org/loc

Galinstan has the potential to replace mercury – one of the most popular liquid metals. However, the easy oxidation of Galinstan restricts wide applicability of the material. In this paper, we report an effective reduction method for the oxidized Galinstan using gas permeable PDMS (polydimethlysiloxane)-based microfluidic channel. The complete study is divided into two parts – reduction of Galinstan oxide and behavior of reduced Galinstan oxide in a microfluidic channel. The reduction of Galinstan oxide is discussed on the basis of static as well as dynamic angles. The contact angle analyses help to find the extent of reduction by wetting characteristics of the oxide, to optimize PDMS thickness and to select suitable hydrochloric acid (HCl) concentration. The highest advancing angle of 155° and receding angle of 136° is achieved with 200 μm thick PDMS film and 37 wt% (weight percent) HCl solution. The behavior of reduced Galinstan oxide is analyzed in PDMS-based coplanar microfluidic channels fabricated using a simple micromolding technique. Galinstan in the microfluidic channel is surrounded by another coplanar channel filled with HCl solution. Due to the excellent permeability of PDMS, HCl permeates through the PDMS wall between the two channels (interchannel PDMS wall) and achieves a continuous chemical reaction with oxidized Galinstan. A Lab VIEW controlled syringe pump is used for observing the behavior of HCl treated Galinstan in the microfluidic channel. Further optimization of the microfluidic device has been conducted to minimize the reoxidation of reduced Galinstan oxide in the microfluidic channel.

1 Introduction

The liquid metals have attracted wide attention for power electronics and electronic devices due to their unique physical properties, such as thermo-conductivity, electrical conductivity and electron mobility. Mercury is the best known of the liquid metals (mercury, gallium, gallium alloy aluminum, tin, *etc.*) and remains the only liquid metal at room temperature. Unfortunately, the toxicity of mercury poses a challenge for its widespread applications. Therefore, it is necessary to find an alternative material for mercury based applications.

Galinstan is a commercially available (from Geratherm Medical AG, Germany) eutectic GaInSn metal alloy (68.5%, 21.5% and 10% by weight, respectively). Considering its outstanding properties such as low melting point (−19 °C), high electrical conductivity (3.46×10^6 S m^{-1}), high boiling point (1300 °C), good thermal conductivity (16.5 W m^{-1} K^{-1}) and ultralow vapor pressure, it can be a suitable replacement for mercury in many applications such as thermometers,[1] coolants,[2] RF micro switches,[3] magneto-hydrodynamic pumps,[4] microvalves,[5] resonators,[6] antennas,[7–12] energy harvesting[13] and tunable frequency selective surfaces (FSS).[14] The working mechanism of tunable FSS devices can be represented by an equivalent circuit based on change in capacitance and/or inductance. This capacitance change depends largely on the movement of Galinstan. Hence, the easy movement of Galinstan is important in the efficient working of many applications.

However, the surface of Galinstan is instantly oxidized under ambient conditions and it behaves more like a gel rather than a true liquid, adhering to almost any solid surface. This oxide layer behaves like a solid and remains elastic unless it experiences a yield stress. The viscous nature of the oxidized Galinstan originates from gallium oxide (Ga_2O_3 and Ga_2O) and it has a significant stickiness problem affecting the easy movement of the liquid metal alloy.[15] In order to overcome this stickiness problem, efforts have been made to avoid the oxidation of Galinstan in recent years. One of the ways to avoid oxidation is to immerse Galinstan in a deoxygenated solution. Hutter *et al.* have used solutions such as polyethylene glycol (PEG) and deoxygenated silicone oil to prevent oxidation of the gallium–indium (Ga–In) alloy.[16]

[a] *School of Mechanical Engineering, Chonnam National University, Gwangju 500757, Republic of Korea. E-mail: mems@chonnam.ac.kr; Fax: +82 62 5300337; Tel: +82 62 5301669*
[b] *Department of Electrical Engineering, The University of Texas at Dallas, Richardson, TX 75080, USA*

† Electronic supplementary information (ESI) available. See DOI: 10.1039/c3lc50952d

According to Liu *et al.* Galinstan behaves like a true liquid metal in sub-ppm oxygen environments.[17] However, this requires a vacuum-sealed hermetic packaging which can be very complex as well as costly. Hence, efforts are made to use either oxidized Galinstan or to remove the complete oxide layer. In order to avoid oxidation of Galinstan, Sivan *et al.* have coated Galinstan droplets with semiconductors or insulators either by rolling them over a powder bed or immersing them in colloidal solutions.[18] Kim *et al.* reported a micro pillar array based super-lyophobic polydimethylsiloxane (PDMS) micro-tunnel for oxidized Galinstan.[19] However, this has a limitation in applying to 3-dimensional structures. Chen *et al.* presented a Teflon coated channel to overcome this sticking of oxidized Galinstan since it is surrounded by Teflon solution.[20] Similarly, Thelen *et al.* have used polyvinyl alcohol (PVA) to stabilize oxide layer of Ga–In liquid metal.[21] Nevertheless, these solutions can obstruct the movement of the oxidized Galinstan. Zrnic *et al.* found that the gallium oxide layer can be removed by treating the surface with diluted HCl solution.[22] As gallium oxide is one of the constituents in the oxidized Galinstan, the oxidized Galinstan can also be reduced using HCl solution. This idea was later implemented by Kocourek *et al.*[23] and Dickey *et al.*.[24] However, the difficulty in both the implementations is the complete immersion of Galinstan droplets into HCl solution which limits its applicability. The chemical aspects of HCl treated Galinstan along with its wetting characteristics are reported by Kim *et al.*[25]

The objective of this paper is to formulate and report a suitable reduction process for the oxidized Galinstan in Galinstan movement-based microfluidic applications using PDMS (with high intrinsic permeability to gases).[26–30] The complete study is divided into subsections on contact angle measurements (static and dynamic) and microfluidic applications. Galinstan moving in microfluidic channels can be constantly maintained in a true liquid phase at room temperature when it is treated continuously by an HCl solution filled coplanar surrounding channel. In addition, the recovery of the non-wetting characteristics of Galinstan droplets is discussed before and after treating the oxidized Galinstan with various concentrations of HCl solution. Finally, the microfluidic device is further optimized to minimize the reoxidation of reduced Galinstan oxide in microfluidic channels.

2 Reduction of Galinstan oxide and its wetting characteristics

2.1 Static contact angle

The contact angle is an experimentally observable quantity that describes the wetting property of a liquid in contact with a solid surface. It can be quantified using Young's equation[31] as

$$\cos\theta = \frac{\gamma_{SG} - \gamma_{SL}}{\gamma_{LG}} \quad (1)$$

where θ is contact angle; γ_{SG}, γ_{SL}, and γ_{LG} are the surface tension of solid–gas, solid–liquid and liquid–gas interfaces, respectively.

As discussed earlier, diluted HCl solution can be used to remove the gallium oxide layer.[22] Hence, first of all, the effect of HCl solution on PDMS needs to be studied. The details of the study have been discussed in the ESI† (supplementary Fig. S1). According to these results, no noticeable damage of PDMS pillars is observed even after immersing the PDMS pillar-based device in 37 wt% HCl for 60 hours. Therefore, in order to analyse the recovery of the non-wetting characteristics of reduced Galinstan oxide droplets on the PDMS surface, the contact angle changes of oxidized Galinstan droplets are measured before and after the reduction using HCl solution. For this, a PDMS film is placed over HCl solution (200 μl). Galinstan (~8 μl) is dropped on the PDMS surface using a syringe. The droplet formed during the dispensing of Galinstan does not form a spherical shape, resulting in a deformed shape as shown in Fig. 1(A1–A2). This is attributed to the oxidation of the surface of Galinstan.[11,18,25] After the permeation of HCl through the PDMS film, it initiates the reduction of oxidized Galinstan. As the oxide layer is removed, the reduced Galinstan oxide surface (with higher surface tension compared to the oxidized one[25]) attains a true liquid nature, and the deformed shape becomes spherical as shown in Fig. 1(B1–B2) which is the basis of Young's eqn (1). Due to this, there is a noticeable change in the contact angle indicating the change in wetting characteristics of the droplet. Here, the droplet contact angle measurements are performed using a charge-coupled device (CCD) camera (15 frames per second) along with an in-house developed image processing MATLAB program.

However, the time required for the reduction of oxidized Galinstan depends on the permeation of HCl and its reactivity towards the oxide layer. In the case of HCl permeation through the PDMS, the PDMS thickness as well as the concentration of the HCl solution is an important factor. Hence, a detailed study on the effect of thickness and HCl solution concentration variation on permeation and oxidized Galinstan

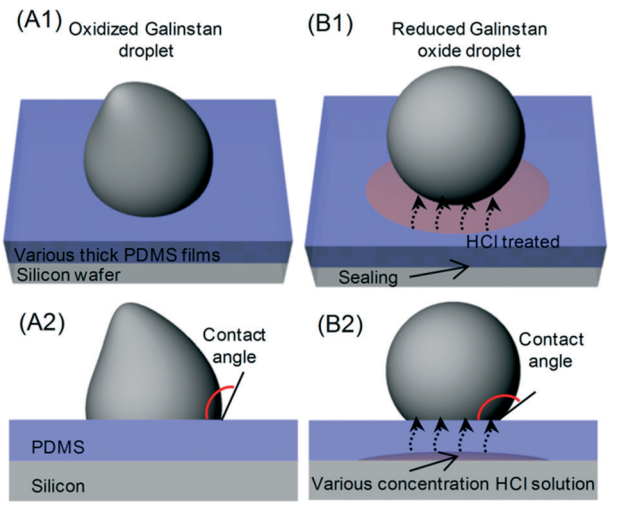

Fig. 1 Sketch of 3-dimensional view and side view of (A1, A2) oxidized Galinstan droplet and (B1, B2) reduced Galinstan oxide droplet using HCl solution.

reduction is necessary. For further validation towards the permeability of PDMS film, the HCl permeation time (through PDMS films of different thickness) is observed using pH paper.

2.1.1 HCl permittivity through PDMS film of different thickness and reduction of oxidized Galinstan. The effect of PDMS thickness on 37 wt% HCl permeation and on the wetting characteristics of reduced Galinstan oxide is shown in Fig. 2(A). It shows the change in contact angle over time for PDMS films having different thicknesses (200 μm–850 μm). Due to the wetting characteristics of oxidized Galinstan, the contact angle of the droplet to the PDMS surface is 125° and increases to 155° after its reduction. The increase in contact angle also indicates the change in wetting characteristics of the droplet. Although the saturated contact angle of the reduced Galinstan oxide is same for all the PDMS films, the rate of increase of contact angle depends on the PDMS thicknesses. Here, the larger the PDMS film thickness, the

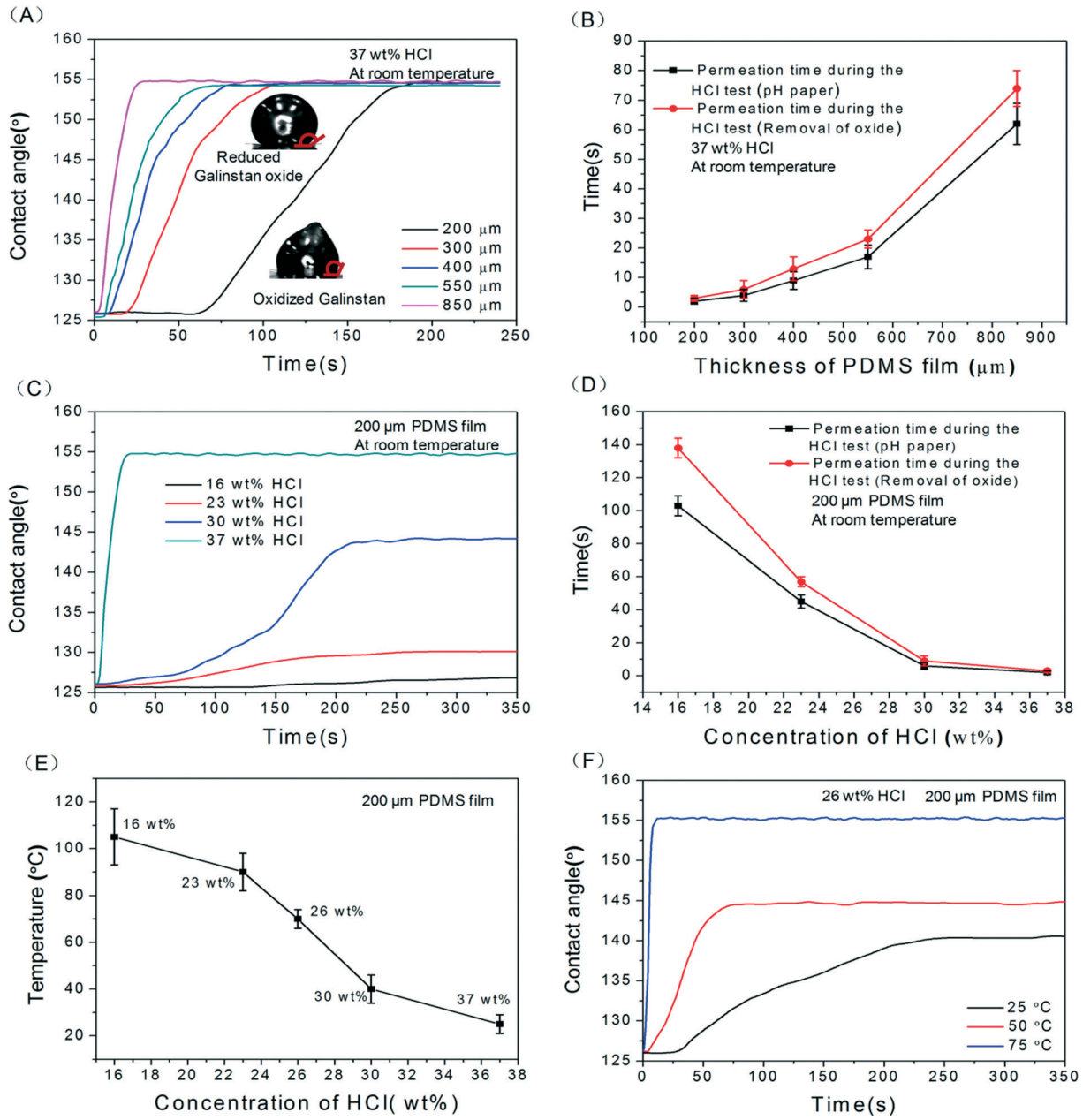

Fig. 2 (A) ~8 μl reduced Galinstan oxide droplet contact angles as a function of time for various PDMS films; (B) the comparison between the permeation time obtained during the reduction of oxidized Galinstan and pH paper test for various PDMS thicknesses; (C) ~8 μl reduced Galinstan oxide droplet contact angles as a function of diffusion time of various HCl concentrations; (D) the comparison between permeation time obtained during the reduction of oxidized Galinstan and pH paper test for various HCl concentrations; (E) optimum temperature for reduction of Galinstan oxide using various concentrations of HCl solution; (F) ~8 μl reduced Galinstan oxide droplet contact angles as a function of time for various operating temperatures.

smaller will be the rate of contact angle variation. In addition to this, the time required to initiate the change of the contact angle also varies with the film thickness. This initial time interval can be considered as the permeation time of HCl through different thicknesses of PDMS films. The permeation time for 37 wt% HCl solution for different thicknesses can be calculated from Fig. 2(A) and compared with the permeation time obtained using pH paper (pH value: 3), as shown in Fig. 2(B). As can be observed in this figure, the permeation time calculated during the reduction is either equal to or greater than the permeation time obtained through the pH paper. This may be due to the fact that the time required for reacting with the Galinstan oxide needs to be included for the previous case of permeation time.

2.1.2 Permittivity of different HCl solutions through PDMS film and its effect on reduction of oxidized Galinstan. In the previous section, 37 wt% HCl solution was used for the reduction of oxidized Galinstan. However, considering the safety issues of using HCl solution (which is generally 37 wt%), efforts were made to study the feasibility of using less concentrated HCl solution for the reduction of oxidized Galinstan droplets placed on 200 μm thick PDMS film. Therefore, the HCl solution was further diluted to 30, 23 and 16 wt%.

Fig. 2(C) shows the change in contact angle of ~8 μl Galinstan droplet (from the oxidized to reduced state) over time for different HCl concentrations with 200 μm thick PDMS film. Because the contact angle represents the wetting characteristics of Galinstan oxide as discussed before, the change in contact angle indicates the extent of reduction. Here, the contact angle of reduced Galinstan oxide varies from ~125° up to ~127°, ~130°, ~145° and ~155° in 16 wt%, 23 wt%, 30 wt% and 37 wt% concentrations of HCl solution respectively. The efficiency of reduction is observed to decrease with increasing HCl dilution. This also reflects the reactivity between oxidized Galinstan and dilute HCl solution. One of the reasons for the less efficient reduction of oxidized Galinstan, using low concentration (<37 wt%) HCl solutions, is the low permeability of these solutions. In addition to this, the reactivity of low concentration (<37 wt%) HCl solutions also decreases with the increase in dilution of HCl solutions. This can be confirmed by observing the rate of change of contact angle for the droplet. Fig. 2(D) shows the comparison between the permeation time of HCl calculated during reduction of Galinstan oxide and the permeation time obtained utilizing pH paper. As can be observed, 37 wt% HCl quickly permeates through the PDMS film compared to other lower concentrations of HCl solution. This can be attributed to the comparatively higher vapor pressure of 37 wt% HCl solution (16 kPa at 20 °C). To summarize this analysis, 37 wt% HCl solution reduces the oxidized Galinstan droplet quickly and completely, allowing it to be a true liquid with non-wetting characteristics even at room temperature.

2.1.3 Temperature effect on permittivity of different HCl solutions and on reduction of oxidized Galinstan. The reduction of oxidized Galinstan depends on two factors – permeation of HCl solution and the reactivity of the solution towards oxidized Galinstan. As discussed before, the permeation time of HCl solution is affected by its vapor pressure. An increase in operating temperature increases the vapor pressure thereby reducing the permeation time. In addition to this, the increase in operating temperature can also enhance the reactivity of HCl solution with Galinstan oxide. To confirm this, oxidized Galinstan was reduced using different concentrations of HCl solution (16–37 wt%) at different operating temperatures. The optimum operating temperature is obtained for the reduction of oxidized Galinstan using different HCl solutions, as shown in Fig. 2(E). The optimum operating temperature is observed to increase with decreasing HCl solution concentration. For 37 wt% HCl solution, complete reduction is observed at room temperature (~25 °C) which increases up to ~105 °C for 16 wt% solution. Here, a lower concentration of HCl requires a higher operating temperature for complete reduction of oxidized Galinstan. On the other hand, a higher operating temperature increases the power consumption as well as the risk factor. Hence, a compromise needs to be made between the selection of HCl concentration and suitable operating temperature. For example, the complete reduction of oxidized Galinstan using 26 wt% HCl solution requires an operating temperature of 75 °C as shown in Fig. 2(F). The permeation time at this temperature is very short (~2–3 s) and the rate of reduction of oxidized Galinstan (*i.e.* reactivity) is also better compared to that at lower operating temperatures (25 °C, 50 °C). In conclusion, it is observed that a higher operating temperature can reduce the permeation time of less concentrated HCl passing through the PDMS film and enhance its ability to reduce the oxidized Galinstan. Therefore, the selection of HCl solution and a suitable operating temperature is advisable.

2.2 Dynamic contact angle

The contact angle of a liquid moving over a surface is termed as the dynamic contact angle. Along with the static contact angle, in order to quantify the wetting property of oxidized Galinstan droplets, the dynamic contact angle (sliding angle and advancing–receding angle) is particularly important. The relation of sliding angle to the advancing and receding contact angles is presented in eqn (2) as:[32]

$$\sin\alpha = \gamma_{LG}\frac{Rk}{mg}\left[\cos\theta_{rec} - \cos\theta_{adv}\right] \quad (2)$$

where α is sliding angle; m is mass of the droplet; θ_{rec} is receding contact angle; θ_{adv} is advancing contact angle; and R and k are a length scale and shape constant for the contour of the droplet respectively (R is generally taken as the droplet radius and k is a fitting parameter based on the experimental data).

2.2.1 Sliding angle. The measurements of sliding angles are carried out on 200 μm thick PDMS film placed on different HCl solutions (16–37 wt%). HCl being volatile in nature will permeate through the PDMS film. After waiting for 3–5 minutes, Galinstan droplets of different volumes are dropped on to the PDMS surface. Due to the presence of HCl

molecules, the oxidized Galinstan will be reduced at the oxide layer thereby affecting its wetting characteristics. Here, the extent of reduction depends on the HCl concentration. Later, the PDMS film is tilted (using the conventional tilted plate technique) at different angles to study the sliding angle of the reduced Galinstan oxide.

Out of all the different concentrations of HCl solutions (16–37 wt%), only 37 wt% HCl completely reduces the oxidized Galinstan at room temperature. Although 30 wt% HCl solution somehow reduces the oxide layer, the oxide removal is incomplete. The contact angle measured for the incompletely reduced oxidized Galinstan is ~145° (Fig. 2(C)). Hence, the sliding angle for the completely reduced Galinstan oxide (using 37 wt% HCl solution) is relatively smaller compared to incompletely reduced Galinstan oxide (using 30 wt% HCl solution). Although the existence of a partial oxide layer makes it adhere to the PDMS surface, the effect of gravity on the Galinstan droplet will overcome the adhesive force and result in sliding of the droplet on a tilted stage with the increase in angle of tilting. Fig. 3 shows a graph depicting the relationship between Galinstan droplet volume and its sliding angle on PDMS with 37 wt% and 30 wt % HCl solution. As can be observed in the figure, the sliding angle of the Galinstan droplet decreases with increasing volume. However, for less concentrated HCl solution (<30 wt%), the effect of gravity on incompletely reduced Galinstan oxide droplets could not overcome the adhesive force even when the tilting angle reached 90° and hence the sliding angle does not exist. For this study, it can be said that 37 wt% HCl solution helps in complete reduction of the oxidized Galinstan and allows fast recovery of non-wetting characteristics. The result is found to be identical to the conclusion discussed previously.

2.2.2 Advancing and receding angle. Analysis of the advancing and receding contact angles has been carried out by adding and removing Galinstan from a droplet using the syringe. For this, Galinstan is continuously dropped on a 200 μm thick PDMS film (covering different HCl solutions) until it reached the maximum volume of 40 μl allowed by CCD camera capturing. After that, the Galinstan is returned back to the syringe. Here, the addition or removal rate of Galinstan is 0.5 μl s^{-1}.

The variation in the advancing and receding contact angles of the Galinstan droplet on the PDMS with various HCl solutions (0–37 wt%) is shown in Fig. 4. During continuous addition of Galinstan, the oxide layer is continuously replaced by unoxidized Galinstan and hence the contact angle (~155°) remains constant throughout the adding process for various concentrations of HCl solution. However the contact angle of oxidized Galinstan is 125° before HCl treatment as shown in Fig. 2(A). This can be explained by the fact that the oxide layer is formed instantly after the Galinstan droplet comes into contact with air and the static contact angle changes from 155° (for unoxidized Galinstan) to 125° (for oxidized Galinstan). For less concentrated HCl solution (<30 wt%), the receding angle appears very low (~60°, ~41°, ~22° and ~6° in 26 wt%, 23 wt%, 16 wt% and 0 wt% conditions respectively) due to incomplete or absence of reduction (supplementary Fig. S3, ESI†). The receding angle would have been even lower than 6° if the measurement had not been ended prematurely by the liquid disconnection during the receding (removal) process. For 30 wt% concentration of HCl solution, the contact angle decreased to a minimum value (96°) and increased to ~116° with removal of Galinstan. This may be due to incomplete reduction of Galinstan oxide surface. The contact angle will increase until the suction force overcomes gravity as well as the adhesive force of the reduced Galinstan oxide droplet, and reaches a maximum value during the receding process. It is observed that the highest concentration of HCl solution makes the smallest Galinstan

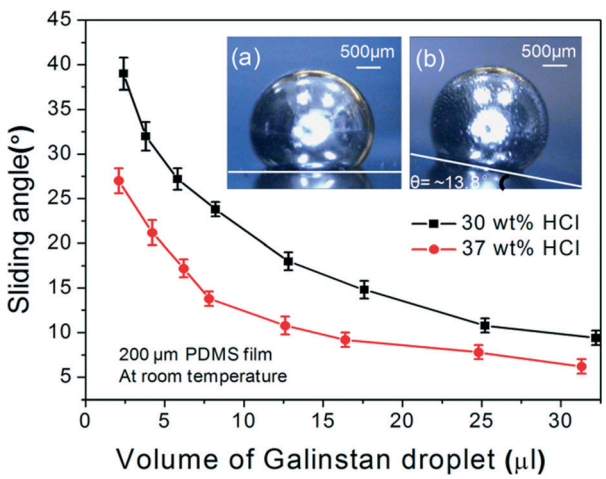

Fig. 3 Reduced Galinstan oxide droplet sliding angles on PDMS film with 37 wt% and 30 wt% HCl solutions: (a) reduced Galinstan oxide droplet (12.5 μl) placed on level plate and (b) sliding on tilted plate.

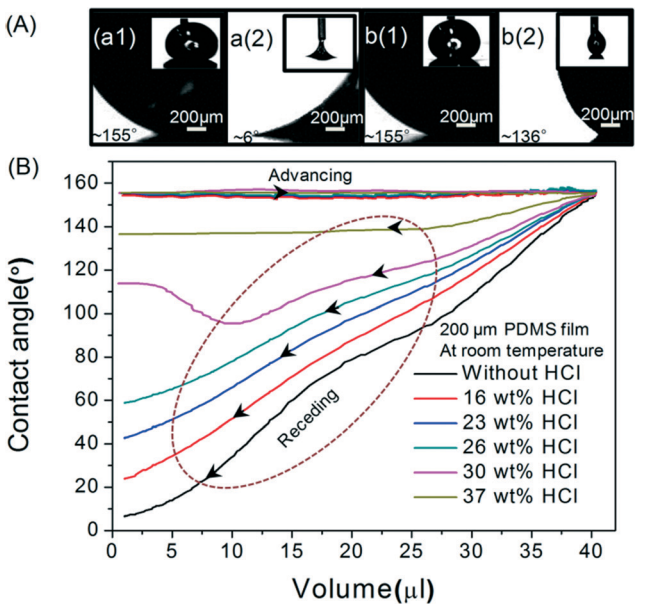

Fig. 4 (A) Photograph of advancing angle and receding angle for oxidized Galinstan (a1, a2) and reduced Galinstan oxide (b1, b2) respectively; (B) Galinstan droplet advancing and receding angle on PDMS film with various concentrations of HCl solution.

droplet contact angle hysteresis (difference value ~19° between advancing angle ~155° and receding angle ~136° for 37 wt% HCl solution) and allows recovery of its non-wetting characteristics at room temperature. Based on the above discussion, it can be concluded that the reduction process of oxidized Galinstan depends on the HCl concentration. Therefore, the extent of reduction deteriorates with a decrease in HCl concentration.

3 Reduced Galinstan oxide in coplanar microfluidic channel

3.1 Realization of microfluidic channel

To demonstrate the behavior of reduced Galinstan oxide in a micro-channel, a coplanar microfluidic channel based PDMS device was designed. The Galinstan containing channel is surrounded by a channel filled with HCl solution. As mentioned before, the HCl concentration as well as the thickness of the interchannel PDMS wall can influence the oxide removal from oxidized Galinstan. After carefully studying the permeability of various concentrations of HCl solution through PDMS films of different thicknesses, the complete reduction of the oxidized Galinstan at room temperature led to the interchannel wall of thickness 200 μm for 37 wt% HCl solution.

Based on the above analysis, the coplanar microfluidic channel device is fabricated using conventional micro-molding technology as shown in Fig. 5. The coplanar microfluidic channel mold is made from SU-8 2050 photoresist (PR) on a silicon wafer. PDMS solution is coated on the coplanar microfluidic channel-mold using standard rapid prototyping methods. After curing, the top PDMS based coplanar microfluidic channel layer is gently peeled off from the mold. The PDMS layer (thickness: 3 mm) has two coplanar channels (cross-sectional area: 600 μm width, 100 μm height) containing 5 ports (diameter: 2.4 mm) to inject Galinstan as well as HCl solution and to apply air pressure for driving the Galinstan droplet. After oxygen plasma activation,[33,34] the PDMS channel layer and the glass slide (as foundation base) are bonded together to complete the channel formation. After fabrication, an experimental setup comprising a CCD camera system and Lab VIEW controlled syringe pump is used to characterize the behavior of reduced Galinstan oxide in the microfluidic channel (supplementary Fig. S4, S5 and supporting video SV1, ESI†). This reduced Galinstan oxide behavior depends on air pressure and the flow rate. For characterizing and enhancing the Galinstan feasibility for electronic device applications like FSS, the conditions in which the Galinstan is filled into the microfluidic channel, separated and later moved; and the accurate movement of a reduced Galinstan oxide droplet using a Lab VIEW controlled syringe pump are necessary.

3.2 Behavior of reduced Galinstan oxide in the microfluidic channel

3.2.1 Reduction of Galinstan oxide in the microfluidic channel. The oxidized Galinstan can easily adhere to the channel wall and it cannot move easily in the microfluidic channel. Oxidized Galinstan has an irregular shape due to its wetting characteristics. Hence, the reduction of this oxidized Galinstan is necessary for its easy movement. As discussed before, 37 wt% HCl solution helps in complete reduction even at room temperature. Hence, the coplanar microfluidic channel is filled with 37 wt% HCl solution so that it permeates through the interchannel wall and reduces the oxidized Galinstan. The permeation time of HCl through the PDMS channel wall is determined by recording the shape change of Galinstan (from the oxidized to reduced state) before and after 37 wt% HCl solution treatment in the microfluidic channel.

The reduced Galinstan oxide seems to behave like a true liquid. The time required for the permeation of HCl (37 wt%)

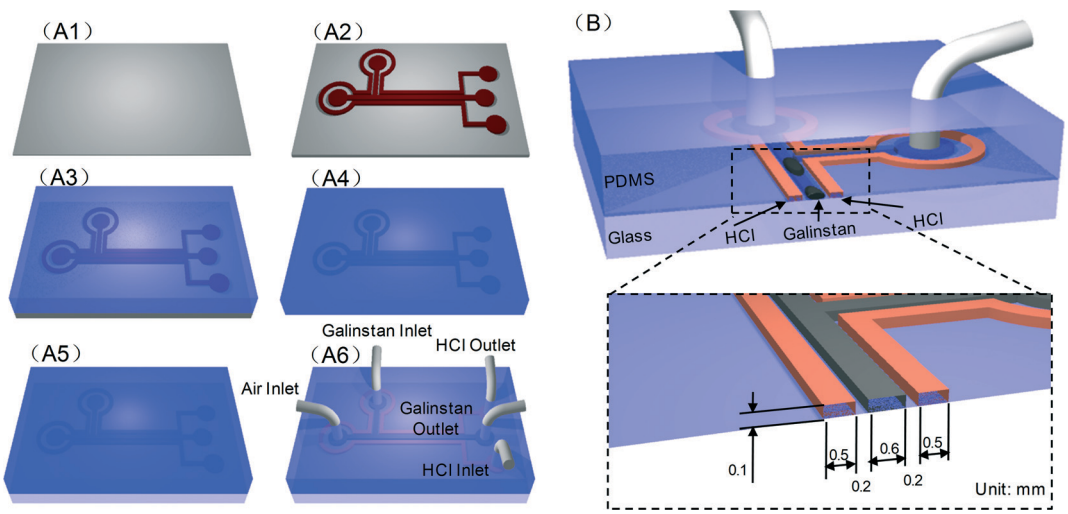

Fig. 5 Fabrication sequence of PDMS channel: (A1) silicon wafer, (A2) SU-8 PR mold on Si wafer, (A3) PDMS coating, (A4) PDMS peeled off from the mold, (A5) PDMS–Glass bonding, (A6) injection of Galinstan in microfluidic channel surrounded by another coplanar channel filled with HCl solution; (B) cross-section of structure and channel size.

through the 200 μm thick PDMS interchannel wall and to reduce the oxidized Galinstan is ~300 s (supplementary Fig. S6, ESI†). The longer duration required for permeation as well as the reduction of oxidized Galinstan in the microfluidic channel compared to the complete reduction of oxidized Galinstan placed on 200 μm PDMS film is due to the limited surface area for the reaction (area: 126 mm length, 0.1 mm height).

3.2.2 Separating and driving. The dependence on applied air pressure for the separation as well as movement of reduced Galinstan oxide into the microfluidic channel surrounded by a coplanar channel containing 37 wt% HCl solution is shown in Fig. 6. Here, Galinstan is continuously injected into the channel and initially gets oxidized and later reduced (removal of oxide layer) due to HCl permeation. The reduced Galinstan oxide is then separated into small droplets at the "T" junction by providing air pressure from the other side (supporting video SV2, ESI†). The inset image Fig. 6(a) indicates that the separation of ~0.15 μl Galinstan droplet requires about 1.7 kPa pressure difference at the "T" junction. However, the pressure difference required to move the same volume of Galinstan droplet is only 1.2 kPa, as shown in the inset image Fig. 6(b). Similarly, for all the droplet volumes higher pressure is required for separating Galinstan into small droplets than moving these droplets in the microfluidic channel. This may be due to fact that during separation, two simultaneous resistive forces (intra-molecular viscous force and inter-molecular adhesive force between Galinstan and the channel wall) need to be overcome; whereas during movement of a Galinstan droplet, only the inter-molecular adhesive force needs to be overcome. Moreover, it can be observed in the plot that the slope of applied air pressure for separation and movement is similar, stressing the fact that the viscous force remains constant but the inter-molecular resistive force depends on the contact area between the surface of the Galinstan droplet and the channel walls.

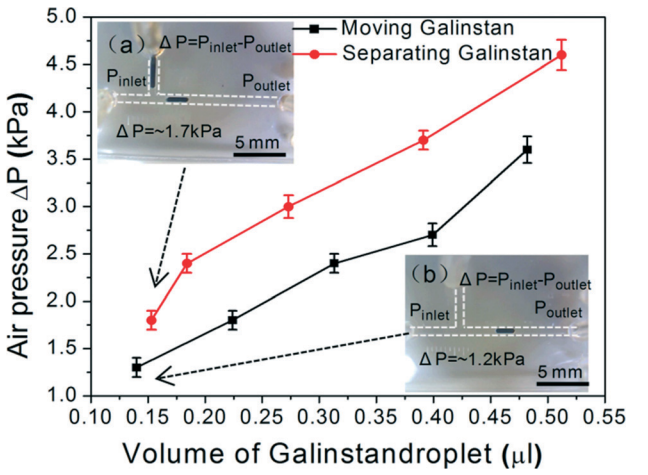

Fig. 6 Separating and moving a reduced Galinstan oxide droplet in a microfluidic channel and its dependence on pressure; photographs (a–b) of separation and movement of reduced Galinstan oxide droplet.

3.2.3 Reoxidation of reduced Galinstan oxide. HCl is a high-vapor pressure liquid. Due to its high vapor pressure, it is quite volatile under ambient conditions and escapes into the environment. One of the ways to reduce the vaporization of HCl is either to cover the ports and surface with glass (Fig. 7) or coat the complete device with a transparent acid-resistant material such as wax, Parafilm® or Teflon (supplementary Fig. S9, ESI†).

Due to the non-wetting characteristics of the reduced Galinstan oxide droplet using 37 wt% HCl solution as discussed before, the minimum pressure required to drive the Galinstan droplet offers information about the absence or presence of the oxide layer and in turn helps to measure the reoxidation time of the reduced Galinstan oxide. The reoxidation time is measured by optimizing the air pressure required to drive the Galinstan at different times under various conditions.

Fig. 7 shows the required pressure difference to drive the reduced Galinstan oxide droplet (0.15 μl) as a function of reoxidation time under various conditions (absence/presence of HCl solution in the microfluidic channel; opening or closing the HCl inlet and outlet; covering glass present on PDMS channel or not). Firstly, the Galinstan droplet (0.15 μl) was moved in the channel when the pressure difference reached ~1.2 kPa (Fig. 7(A-a1)). The required pressure difference to drive the Galinstan droplet increases with time until the Galinstan droplet shape is changed (Fig. 7(A-a2)). This

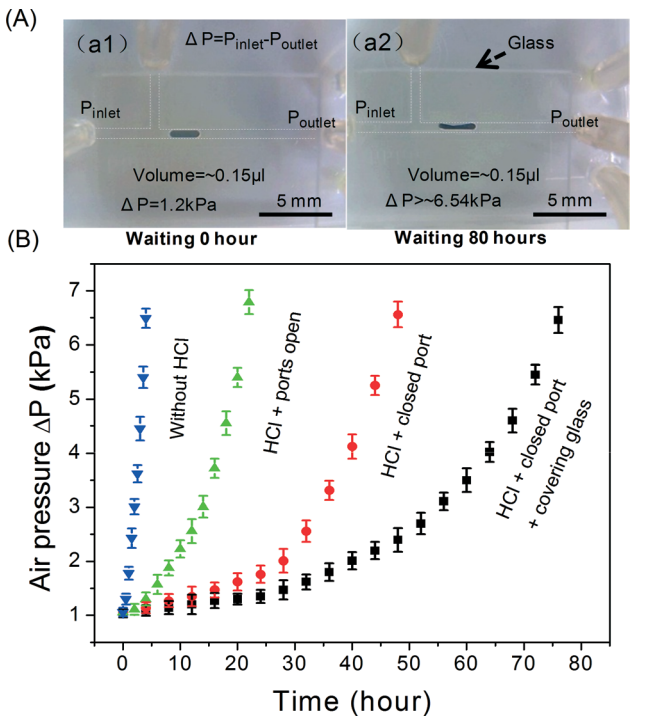

Fig. 7 (A) Photographs a1–a2 showing the initial and final (after 80 hours) shape of reduced Galinstan oxide for the conditions in which HCl solution is present in the microfluidic channel, the HCl inlet and outlet are closed, and glass is covering the PDMS channel surface; (B) air pressure as a function of reoxidation time under various conditions.

change in shape of the droplet indicates the presence of the oxide layer and hence, shows a variation in the wetting characteristics. As can be observed from Fig. 7(B), the reoxidation time is 4 hours, 20 hours and 48 hours respectively under the first set of conditions (removing HCl solution from the microfluidic channel), second conditions (leaving the HCl solution in the microfluidic channel and opening the HCl inlet and outlet) and third conditions (leaving the HCl solution in microfluidic channel and closing the HCl inlet and outlet). For fourth set of conditions (leaving the HCl solution in the microfluidic channel, closing the HCl inlet and outlet, and covering the PDMS channel surface with glass to reduce evaporation of HCl), the Galinstan droplet shape is changed when a pressure difference of ~6.54 kPa is applied to drive it after 80 hours (Fig. 7(A-a2)). The reason is that the Galinstan droplet is oxidized and adheres to the inner wall after 80 hours. The volatilization rate of HCl under the fourth set of conditions is lower than that under the previous three conditions. Therefore, the time for which the Galinstan droplet maintains a true liquid phase and a stable structure in the microfluidic channel is the longest.

3.2.4 Dynamic analyses of reduced Galinstan oxide at different applied air pressure. The main objective of removing the oxidized Galinstan layer in this study is to retain the non-wetting characteristics of Galinstan for its easy movement in a microchannel environment. The easy as well as precise movement of Galinstan is important for the efficient working of many applications. Therefore to demonstrate the precise position control of reduced Galinstan oxide, efforts have been made to study the linear and reciprocating motion.

To control the movement (linear and reciprocating motion) of Galinstan droplets, an experimental setup including a syringe pump, computer along with Lab VIEW data acquisition system and CCD camera is used. The details of this setup are provided in the supplementary information (supplementary Fig. S4, S5 and supporting video SV1, ESI†). In brief, the microchannel is connected to a Lab VIEW controlled syringe pump. This pump can generate the necessary pressure difference to move the Galinstan droplet in reciprocating (forward or reverse) directions. Latter, the velocities of the reduced Galinstan oxide droplet as a function of time with various air flow rates are obtained by using a video process.

Fig. 8(A) shows the velocities of linear movement of reduced Galinstan oxide droplets (~0.15 μl) with various air flow rates (0.6, 1.2, 1.8, 2.4 and 3.0 ml min^{-1}) controlled by the syringe pump (supporting video SV3, ESI†). At first, the air is injected into the inlet of the microfluidic channel at particular flow rates (mentioned above) and used for driving the droplet. The reduced Galinstan oxide droplet moves only when the pressure difference exceeds a certain value depending on volume of the droplet (for example, ~0.15 μl requires 1.2 kPa pressure difference) as discussed before. The velocity of the droplet increases with time and tends to saturate later. This saturation of droplet velocity may be due to the fixed air flow rate and the constant resistive (intermolecular adhesive) force on the movement of the reduced Galinstan oxide droplet. As expected, a larger flow rate results in a higher value for maximum velocity of the reduced Galinstan oxide droplet.

As shown in Fig. 8(B), the velocities of reciprocating movement of reduced Galinstan oxide droplets (~0.15 μl) with various air flow rates (3.6, 4.2, 4.8, and 5.4 ml min^{-1}) are obtained and the shape of the curve changed periodically (period T = 4.2 s) (supporting video SV4, ESI†). In first 1/4 T cycle, the velocity of the Galinstan droplet is increased until the direction of the Galinstan droplet is changed. Here, the direction of Galinstan droplet movement is changed by changing the direction of the air flow and there is a delay of 1/4 T between the air flow direction change and the droplet direction change. This delay is due to the time taken for reducing the velocity of the droplet before changing its direction. After the change in direction, the velocity of the droplet exhibits a negative value in the plot. At this moment, the negative value of velocity is nothing but the change in direction of movement. The velocity remains at the maximum value until the direction of Galinstan flow is changed again. Because of the existence of flow resistance (inter-molecular adhesive force between Galinstan and the channel wall), the curve exhibits an irregular shape. As can be observed in the

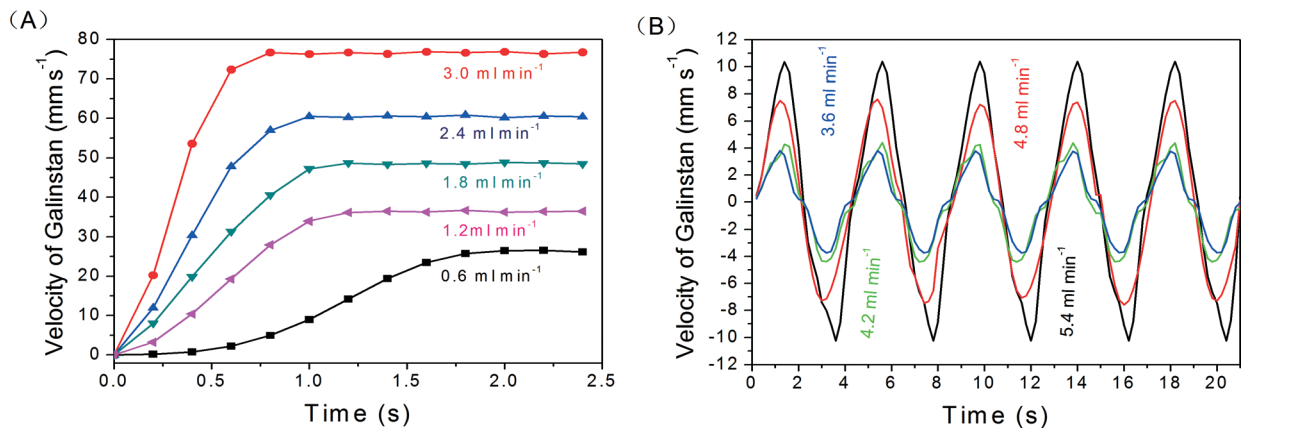

Fig. 8 Velocity of reduced Galinstan oxide droplet for (A) linear movement with various flow rates; (B) reciprocating movement with various flow rates.

Fig. 8(B), the maximum value for velocity of the droplet is much smaller compared to Fig. 8(A). This can be explained as the variation in experimental conditions necessary for the movement in reciprocating (back-and-forth) directions. Here, the pressure needs to be applied at both the end ports compared to the single end port pressure application for the experimental data shown in Fig. 8(A). Fig. 8 shows that our design not only controls the precise movement of the droplet but also can reduce the device response time by using higher flow rates. These higher flow rates result in the higher velocity of reduced Galinstan oxide droplets and enhance the overall performance behavior. However, the use of Galinstan in applications requiring its movement like coolants,[2] RF micro switches[3]or FSS[14] needs further optimization.

4 Conclusions

In this study, coplanar microfluidic channels using gas permeable PDMS are applied for surface reduction of oxidized Galinstan. The microfluidic channel injected Galinstan is surrounded by another HCl-filled coplanar channel. The interchannel PDMS wall thickness (200 μm) is optimized after the HCl permeability study through different thicknesses of PDMS films. Due to the good permeability of PDMS, 37 wt% HCl can pass through the interchannel PDMS wall easily to achieve continuous chemical reduction of oxidized Galinstan. Considering safety while using HCl solution, the efforts are made to find an optimum operating temperature to completely reduce the Galinstan oxide layer using a lower HCl concentration (26 wt% instead of 37 wt%). The optimum temperature for the complete reduction using 26 wt% HCl solution is measured to be 75 °C. Based on this detailed analysis, simple microfluidic coplanar channels are fabricated using conventional micro-molding technology.

The Lab VIEW controlled syringe pump system is used for controlling the movement of HCl treated Galinstan in microfluidic channels in a common microfluidic environment. The microfluidic device is further optimized to reduce the reoxidation rate of reduced Galinstan oxide. Finally, we have obtained the velocities of linear and reciprocating motion of Galinstan droplets with various air flow rates. The experimental results demonstrate that this microfluidic platform can easily reduce the oxidized Galinstan and make HCl treated Galinstan oxide a non-wetting liquid metal alloy.

The present study is applicable mostly for droplets as our intention was to realize a variable capacitor and tunable FSS. Both these applications employ exact control of the droplet position. The change in capacitance depends largely on the position or the shape of Galinstan and this variable capacitance forms one of the building blocks of tunable FSS devices.

Acknowledgements

This work was supported by the WCU (World Class University) program through the National Research Foundation of Korea (NRF) grant funded by the Korean government (MEST) (no. R 32-20087). The National Research Foundation of Korea (NRF) grant through the Korean government (MEST) (no. 2012R1A2A2A01014711) has also funded in the present study.

References

1 S. R. Schreiber, M. M. Minute, G. M. Tornese, R. M. Giorgi, M. R. Duranti, L. M. Ronfani and E. M. Barbi, *Pediatr. Emerg. Care*, 2013, **29**, 97–199.
2 K. Mohseni and E. S. Baird, *Nanosc. Microsc. Therm.*, 2007, **11**, 99–108.
3 P. Sen and C. J. Kim, *IEEE Trans. Ind. Electron.*, 2009, **56**, 1314–1330.
4 W. Irshad and D. Peroulis, *Proceedings of PowerMEMS 2009*, Washington DC, 2009, pp. 127–129.
5 N. Pekas, Q. Zhang and D. Juncker, *J. Micromech. Microeng.*, 2012, **22**, 097001.
6 X. G. Liu, L. P. B. Katehi and D. Peroulis, *Microwave Conference, 2009. APMC 2009. Asia Pacific*, Singapore, 2009, pp. 131–134.
7 J. H. So, J. Thelen, A. Qusba, G. J. Hayes, G. Lazzi and M. D. Dickey, *Adv. Funct. Mater.*, 2009, **19**, 3632–3637.
8 S. Cheng and Z. G. Wu, *Lab Chip*, 2010, **10**, 3227–3234.
9 M. Kubo, X. Li, C. Kim, M. Hashimoto, B. J. Wiley, D. Ham and G. M. Whitesides, *Adv. Mater.*, 2010, **22**, 2749–2752.
10 S. Cheng and Z. G. Wu, *Adv. Funct. Mater.*, 2011, **21**, 2282–2290.
11 S. Cheng and Z. G. Wu, *Lab Chip*, 2012, **12**, 2782–2791.
12 A. A. Nawaz, X. Mao, Z. S. Stratton and T. J. Huang, *Lab Chip*, 2013, **13**, 1457–1463.
13 T. Krupenkin and J. Ashley Taylor, *Nat. Commun.*, 2011, **2**, 1454.
14 M. Li, B. Yu and N. Behdad, *IEEE Microw. Wireless Compon. Lett.*, 2010, **8**, 423–425.
15 F. Scharmann, G. Cherkashinin, V. Breternitz, C. Knedlik, G. Hartung, T. Weber and J. A. Schaefer, *Surf. Interface Anal.*, 2004, **36**, 981–985.
16 T. Hutter, W. C. Bauer, S. R. Elliott and W. T. S. Huck, *Adv. Funct. Mater.*, 2012, **22**, 2624–2631.
17 T. Y. Liu, P. Sen and C. J. Kim, *J. Microelectromech. Syst.*, 2012, **21**, 443–450.
18 V. Sivan, S.-Y. Tang, A. P. O'Mullane, P. Petersen, N. Eshtiaghi, K. Kalantar-zadeh and A. Mitchell, *Adv. Funct. Mater.*, 2013, **23**, 144–152.
19 D. Kim, D. W. Lee, W. Choi and J. B. Lee, *Micro 2012 IEEE 25th International Conference on Electro Mechanical Systems (MEMS)*, Paris, 2012, pp. 1005–1008.
20 C. H. Chen and D. Peroulis, *IEEE Trans. Microw. Theory Techn.*, 2007, **55**, 2919–2929.
21 J. Thelen, M. D. Dickey and T. Ward, *Lab Chip*, 2012, **12**, 3961–3967.
22 D. Zrnic and D. S. Swatik, *J. Less-Common Met.*, 1969, **18**, 67–68.
23 V. Kocourek, C. Karcher, M. Conrath and D. Schulze, *Phys. Rev. E: Stat., Nonlinear, Soft Matter Phys.*, 2006, **74**, 026303.

24 M. D. Dickey, R. C. Chiechi, R. J. Larsen, E. A. Weiss, D. A. Weitz and G. M. Whitesides, *Adv. Funct. Mater.*, 2008, **18**, 1097–1104.
25 D. Kim, P. Thissen, G. Viner, D. W. Lee, W. Choi, Y. J. Chabal and J. B. Lee, *ACS Appl. Mater. Interfaces*, 2013, **5**, 179–185.
26 T. C. Merkel, V. I. Bondar, K. Nagai, B. D. Freeman and I. Pinnau, *J. Polym. Sci., Part B: Polym. Phys.*, 2000, **38**, 415–434.
27 R. B. Qi, Y. J. Wang, J. D. Li, C. W. Zhao and S. L. Zhu, *J. Membr. Sci.*, 2006, **280**, 545–552.
28 S. Takegami, H. Yamada and S. Tsujii, *J. Membr. Sci.*, 1992, **75**, 93–105.
29 Y. Zhang, M. Ishida, Y. Kazoe, Y. Sato and N. Miki, *IEEJ Trans. Electr. Electron. Eng.*, 2009, **4**, 442–449.
30 H. X. Rao, F. N. Liu and Z. Y. Zhang, *J. Membr. Sci.*, 2007, **303**, 132–139.
31 J. Lee, H. Moon, J. Fowler, T. Schoellhammer and C. J. Kim, *Sens. Actuators, A*, 2002, **95**, 259–268.
32 C. G. L. Furmidge, *J. Colloid Sci.*, 1962, **17**, 309–324.
33 M. K. Chaudhury and G. M. Whitesides, *Langmuir*, 1991, **7**, 1013–1025.
34 W. R. Childs, M. J. Motala, K. J. Lee and R. G. Nuzzo, *Langmuir*, 2005, **21**, 10096–10105.